

Excitation of Cy5 in self-assembled lipid bilayers using optical microresonators

Lindsay M. Freeman,¹ Su Li,¹ Yasaman Dayani,¹ Hong-Seok Choi,¹ Noah Malmstadt,¹ and Andrea M. Armani^{1,2,a)}

¹Mork Family Department of Chemical Engineering and Materials Science, University of Southern California, 3651 Watt Way, Los Angeles, California 90089, USA

²Ming Hsieh Department of Electrical Engineering-Electrophysics, University of Southern California, 3651 Watt Way, Los Angeles, California 90089, USA

(Received 25 January 2011; accepted 20 March 2011; published online 6 April 2011)

Due to their sensitivity and temporal response, optical microresonators are used extensively in the biosensor arena, particularly in the development of label-free diagnostics and measurement of protein kinetics. In the present letter, we investigate using microcavities to probe molecules within biomimetic membranes. Specifically, a method for self-assembling lipid bilayers on spherical microresonators is developed and the bilayer-nature is verified. Subsequently, the microcavity is used to excite a Cy5-conjugated lipid located within the bilayer while the optical performance of the microcavity is characterized. The emission wavelength of the dye and the optical behavior of the microcavity agree with theoretical predictions. © 2011 American Institute of Physics.

[doi:10.1063/1.3576908]

Whispering gallery mode microcavities were initially developed for telecommunications and fundamental physics applications, such as add-drop filters, low threshold lasers, and cavity quantum electrodynamics investigations.¹ In a whispering gallery mode device, the light is partially confined in circular orbits by total internal reflection [Fig. 1(a)]. As a result of their long photon lifetimes or high quality factors (Q) which result in large build-up intensities, whispering gallery mode resonators have played a pivotal role in many of the recent demonstrations of ultralow threshold lasers, nonlinear optics, and physics discoveries.

Recently, these devices have transitioned to the biological and chemical sensor arena.² A small portion of the optical field extends into the environment forming an evanescent tail, which interacts with molecules, enabling detection, and excitation of fluorescent probes. Therefore, although the majority of sensor research has focused on label-free detection strategies for diagnostics, a whispering gallery mode device is ideally suited to perform fluorescent label-based detection as well.³ For example, if appropriately functionalized, these devices will be ideally suited to study the mobility of proteins within a biomimetic coating,^{3,4} like a lipid bilayer, or investigate the photodynamics of fluorescent proteins and molecules within these coatings.⁵ While there are several microscopy and spectroscopy techniques which can also be used to perform these experiments, resonant cavities have significantly improved temporal resolution. Previous research using optical microcavities to excite fluorescent molecules has focused on cavity quantum electrodynamics applications and fundamental studies of the interactions of large fluorescent nanoparticles with the resonant cavity with limited experimental efforts combining biomimetic surface coatings with surface cavity excitation techniques.⁶

To experimentally verify the ability of the resonant cavity method to excite and detect dye molecules in a biologi-

cally relevant environment, a spherical resonant cavity was combined with a self-assembled lipid bilayer coating. Solid-supported lipid bilayers, which are approximately 5 nm thick, have been shown to accurately model cell membranes, and researchers use lipid bilayers in combination with fluorescent microscopy when developing theoretical models for the transport of molecules across the cell membrane.³ During the course of the present work, a new method for self-assembling a lipid bilayer on the surface of a high performance optical device is developed and is demonstrated using ultra high Q microsphere resonators, thereby verifying that this method will enable future generations of experiments in the field of biophysics.

To predict the length of the evanescent field, a series of

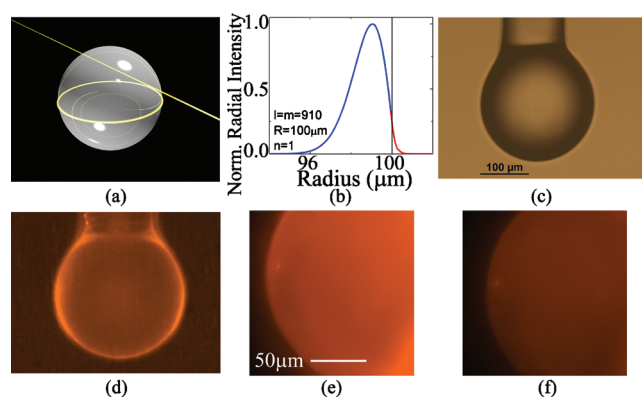


FIG. 1. (Color) Optical resonant cavity excitation of Cy5-conjugated lipids. (a) A rendering of a spherical resonant microcavity highlighting the location of the optical field. (b) The optical field intensity inside (blue line) and outside (red line) of the cavity with a 5 nm bilayer at 980 nm. The decay length is approximately 100 nm. The n , l , and m represent the radial, polar, and azimuthal mode number, respectively. (c) An optical micrograph of the silica microsphere microcavity before lipid bilayer attachment. (d) A wide-field fluorescence micrograph of the microcavity after lipid bilayer attachment. (e) A close-up fluorescence micrograph of the microcavity surface in buffer. (f) The same microcavity after the addition of a fluorescence quenching agent.

^{a)}Author to whom correspondence should be addressed. Electronic mail: armani@usc.edu.

finite element method simulations (COMSOL Multiphysics) are performed.^{7,8} The mesh size of the simulation in the region of the optical field is $0.016 \mu\text{m}^2$ (area divided by no. of mesh). The field distribution is modeled assuming a $200 \mu\text{m}$ diameter spherical resonant cavity with a 5 nm thick bilayer. The refractive index of the microsphere (silica) was taken from the COMSOL library and the refractive index of the lipid bilayer was taken from Ref. 9. The percentage of the optical field is determined by $\text{Power}_{\text{In(Silica,Bilayer,Air)}}/\text{Power}_{\text{Tot}}$, where Power_{In} and $\text{Power}_{\text{Tot}}$ represent the portion of the optical power in each region and total optical power in the cavity and its surrounding environment, respectively. The resonant wavelength was set to 633 or 980 nm in each simulation by controlling the azimuthal mode order in the cavity (M). The inset in Fig. 1(b) shows the FEM simulation results for a 5 nm thick lipid bilayer on a microsphere at 980 nm. As can be seen, the evanescent tail is approximately 100 nm. Therefore, based on these simulations, the resonant cavity should interact strongly with fluorophores located in this region.

The spherical resonant cavities are fabricated from standard optical fiber (Newport) using a conventional CO_2 laser reflow method. After device fabrication, the resonant cavity is suspended in a solution of small unilamellar vesicles formed from 1,2-dipalmitoyl-*sn*-glycero-3-phosphocholine and 1,2-dioleoyl-*sn*-glycero-3-phosphocholine, and cholesterol (at a 2:2:1 mass ratio).¹⁰ Additionally, for some experiments, either Texas Red-modified 1,2-dipalmitoyl-*sn*-glycero-3-phosphoethanolamine (TR-DPPE, Invitrogen) or Cy5-1,2-dimyristoyl-*sn*-glycero-3-phosphoethanolamine (Cy5-DMPE) is used (at 0.1 wt % TR-DPPE or 1 wt % Cy5-DMPE). The Cy5-DMPE is synthesized by reaction of 1,2-dimyristoyl-*sn*-glycero-3-phosphoethanolamine (DMPE, Avanti) with the N-hydroxysuccinimidyl ester of Cy5 (Cy5 NHS-ester, GE Healthcare). Over the course of 36 h, the lipid bilayer self-assembles on the surface of the optical resonant cavity through vesicle adsorption and fusion on the microcavity surface.¹¹ The uniformity of the lipid bilayer on the surface of the resonant cavity is verified using fluorescence microscopy by incorporating TR-DPPE into the lipid bilayer [Fig. 1(d)].

The bilayer structure on the microsphere surface is experimentally confirmed. First, a soluble Förster resonance quencher molecule (QSY-7 amine, Invitrogen) is added to the buffer surrounding a microsphere coated with lipids including TR-DPPE. The fluorescence intensity from the sphere drops by 51%, and drops no further upon the addition of increasing quantities of quencher [Figs. 1(e) and 1(f)].⁷ This indicates that the lipids are organized in two distinct leaflets, only one of which is solvent-accessible. A fluorescence recovery after photobleaching experiment is also performed on a separate microsphere. A spot on the surface of the microsphere is bleached by intense focused light to 53% of its initial intensity. This spot recovers to 97% of the initial fluorescence over 20 min, indicating that the lipids are mobile, as expected for a true molecular bilayer.⁷

To verify the interaction of the evanescent field with the lipid bilayer, the quality factor of a lipid bilayer-coated resonant cavity is determined using bilayers containing or not containing Cy5-DMPE. This measurement is performed in both the visible (633 nm) and the near-IR (980 nm) using a pair of single-mode, tunable external cavity continuous wavelength lasers centered at those wavelengths. The lasers

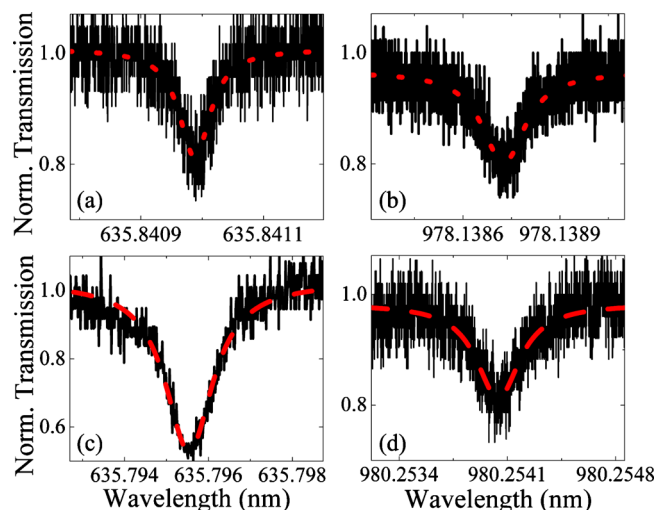


FIG. 2. (Color online) The measurements of the photon lifetime or Q factor, which indicates the interaction strength between the whispering gallery mode and the lipid bilayer. The quality factor was determined from the full-width at half maximum (FWHM, $\Delta\lambda$) of the Lorentzian fit (dashed red line) to the experimental data (solid black line). This measurement was performed using an undoped lipid bilayer at (a) 633 nm and (b) 980 nm, and using a Cy5 conjugated lipid bilayer at (c) 633 nm and (d) 980 nm.

are coupled to the resonant cavities using tapered optical fiber waveguides.^{12,13} Top and side view machine vision systems are used to monitor the gap between the taper and the resonant cavity. Both the intrinsic Q and resonant wavelength of the cavity are determined by monitoring the power transmission spectra on a high speed digitizer. The Q factor ($Q = \omega\tau = \lambda/\Delta\lambda$, where ω =angular frequency, τ =photon lifetime, λ =wavelength, and $\Delta\lambda$ =linewidth) is determined by scanning the wavelength of the single-mode laser and measuring both the resonant power transmission and the loaded linewidth in the undercoupled regime. The intrinsic modal linewidth and hence the intrinsic Q is then computed using a resonator-waveguide coupling model.¹²

The absorption maximum of Cy5 is approximately 650 nm. In the present case, the quality factor is inversely proportional to the material absorption.¹⁴ The precise nature of this dependence can be calculated from the previously described finite element method simulations by determining the intensity of the optical field which interacts with the Cy5-DMPE [Fig. 1(b)]. At 980 nm, the material absorption of the Cy5-DMPE is similar to that of the dye-free lipid bilayer; consequently, the simulations predict the photon lifetime of the device should be the same with or without dye present. In contrast, at 633 nm, the high optical absorption of the Cy5 should reduce the photon lifetime and decrease the measured quality factor. As shown in Fig. 2, the quality factor of the cavity at 633 nm decreases by nearly two orders of magnitude when the Cy5-DMPE is present (1.594×10^7 to 5.308×10^5) while the quality factor at 980 nm remains constant (6.601×10^6 to 3.033×10^6). Therefore, the evanescent tail is strongly overlapping with the lipid bilayer and interacting with the Cy5-DMPE.

To verify that the optical cavity is capable of exciting fluorophores which are embedded in a complex membrane and that it is compatible with conventional high-speed spectroscopy methods, the Cy5 is excited via the evanescent tail of the whispering gallery mode of the optical cavity using a 1.2 mW tunable laser centered at 633 nm. An attenuator was

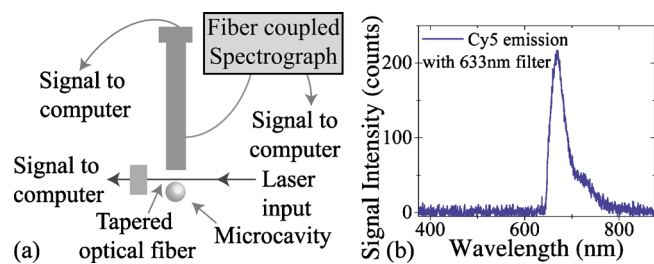


FIG. 3. (Color online) The fluorescent emission spectra of the Cy5 in the lipid bilayer excited using the microcavity. (a) Schematic of test and measurement setup. The evanescent field of the microcavity excites the Cy5-conjugated lipids, and the emission is detected by the spectrograph. The optical power is fiber coupled into and out of the resonant cavity, and the collected fluorescence signal is fiber coupled into the spectrograph. (b) The emission from the Cy5-conjugated lipid bilayer which is excited by the optical microresonator. The peak maximum is located at 670.11 nm. The 633 nm excitation laser is blocked using a filter.

used to reduce the output power on the laser to 200 μW . To measure the emission spectrum of Cy5, a port was added into the side view camera optical column with an integrated beam splitter. As shown in the testing apparatus schematic in Fig. 3(a), a custom adapter was machined to connect the fiber optic cable from the spectrograph (Andor Shamrock spectrograph with a Newton CCD detector) to the optical column (Navitar). The beam splitter allowed approximately 50% of the light to pass and go to the camera while reflecting 50% of the light into the optical fiber which was coupled to the spectrograph. Through a judicious choice of beam-splitter location, the objective focused the back-reflected light precisely onto the face of the optical fiber, thus maximizing this photon collection. Finally, a custom 633 nm filter (Chroma) was inserted between the optical column and the microsphere to block the excitation laser. Using Andor's SOLIS software, data was automatically acquired with a detector exposure time of 3 s.

As shown in Fig. 3(b), the Cy5 dye in the lipid bilayer is efficiently excited using the evanescent field of the microcavity with minimal input power, and the emission spectra is accurately recorded with excellent signal-to-noise ratio. Previous research has shown that Cy5 has an emission wavelength of 670 nm.¹⁵ The peak emission wavelength of Cy5 excited using the optical cavity is 670.11 nm, which is in excellent agreement with previous results. Therefore, the experiments demonstrate that the optical cavity method is able to accurately excite the fluorescent molecules conjugated to lipid bilayers.

In summary, we have proposed and demonstrated the ability of optical resonant cavities to probe fluorescent molecules in self-assembled lipid bilayers. We have performed finite element method simulations of the evanescent field generated by the optical microcavity and verified that the

evanescent tail is approximately 100 nm long, which is ideal for studying proteins within a self-assembled lipid bilayer. We also developed a surface chemistry method for self-assembling a lipid bilayer on the surface of an optical microcavity without degrading the device performance. Finally, we verified the nature of the lipid bilayer, confirming that this method forms a lipid bilayer, and not a multilayer or unorganized lipid structure. We expect that this technique will find numerous applications in both the biological sciences, such as studying passive transport across the cell membranes or interactions between biomolecules and membranes³ and in the development of new types of fluorescent probes and characterizing the interactions of these probes with their immediate environments.⁵

The authors are grateful to Dr. Mark Oxborrow at the National Physical Laboratory (NPL) for helpful discussions regarding finite element method simulation techniques. This work was supported by the National Science Foundation (Grant Nos. DBI-0852581 and ENG-1028440), the Office of Naval Research Young Investigator's Program (Grant No. N00014-09-1-0898), and the National Institutes of Health (Grant Nos. 1R21AG033890 and 1R01ES017034). L. Freeman was supported in part by the Undergraduate Research Associates Program at the University of Southern California. Additional information is available at <http://armani.usc.edu>.

¹K. J. Vahala, *Nature (London)* **424**, 839 (2003).

²X. D. Fan, I. M. White, S. I. Shopoua, H. Y. Zhu, J. D. Suter, and Y. Z. Sun, *Anal. Chim. Acta* **620**, 8 (2008); H. K. Hunt and A. M. Armani, *Nanoscale* **2**, 1544 (2010).

³S. Li, P. Hu, and N. Malmstadt, *Anal. Chem.* **82**, 7766 (2010).

⁴L. V. Schafer, D. H. de Jong, A. Holt, A. J. Rzepiela, A. H. de Vries, B. Poolman, J. A. Killian, and S. J. Marrink, *Proc. Natl. Acad. Sci. U.S.A.* **108**, 1343 (2011).

⁵J. Goedhart, L. van Weeren, M. A. Hink, N. O. E. Vischer, K. Jalink, and T. W. J. Gadella, *Nat. Methods* **7**, 137 (2010).

⁶S. Göttinger, L. D. Menezes, A. Mazzei, S. Kuhn, V. Sandoghdar, and O. Benson, *Nano Lett.* **6**, 1151 (2006); D. J. Norris M. KuwataGonokami, and W. E. Moerner, *Appl. Phys. Lett.* **71**, 297 (1997); J. Topolancik and F. Vollmer, *Biophys. J.* **92**, 2223 (2007).

⁷See supplementary material at <http://dx.doi.org/10.1063/1.3576908> for additional figures and details.

⁸M. Oxborrow, *IEEE Trans. Microwave Theory Tech.* **55**, 1209 (2007); H.-S. Choi, X. Zhang, and A. M. Armani, *Opt. Lett.* **35**, 459 (2010).

⁹S. Schouten, P. Stroeve, and M. L. Longo, *Langmuir* **15**, 8133 (1999).

¹⁰V. P. Torchilin and V. Weissig, *Liposomes: A Practical Approach*, 2nd ed. (Oxford University Press, Oxford, 2003), p. 396.

¹¹A. A. Brian and H. M. McConnell, *Proc. Natl. Acad. Sci. U.S.A.* **81**, 6159 (1984).

¹²S. M. Spillane, T. J. Kippenberg, O. J. Painter, and K. J. Vahala, *Phys. Rev. Lett.* **91**, 043902 (2003).

¹³B. E. Little, J. P. Laine, and H. A. Haus, *J. Lightwave Technol.* **17**, 704 (1999).

¹⁴D. W. Vernooy, V. S. Ilchenko, H. Mabuchi, E. W. Streed, and H. J. Kimble, *Opt. Lett.* **23**, 247 (1998).

¹⁵L. L. Wang, A. K. Gaigalas, and V. Reipa, *Biotechniques* **38**, 127 (2005).